

# Preparation of High Value Added Chemicals by Layered G-C<sub>3</sub>N<sub>4</sub> Photocatalytic Oxidation of Glucose

Yan Li<sup>1,\*</sup>, Yutian Xu<sup>1</sup>, Dan Zheng<sup>1</sup>

<sup>1</sup>Secondary Vocational Education Department of Weifang Engineering Vocational College, No. 4139, Linglongshan South Road, Qingzhou, Shandong Province, 262500 Qingzhou, China

**Abstract.** This study used cyanamide as the precursor and SiO<sub>2</sub> as the template to prepare a layered structure g-C<sub>3</sub>N<sub>4</sub>, and characterized its crystal structure, morphology, optical performance, and electrochemical performance. Photocatalytic oxidation experiments were conducted on biomass derivatives (glucose). Orthogonal experiments were used to study the effects of factors such as illumination time, catalyst concentration, and photocurrent on photocatalytic reactions, and the reaction mechanism was explored. The product was qualitatively analyzed by gas chromatography-mass spectrometry (GC-MS) and quantitatively analyzed by High-performance liquid chromatography (HPLC). The results showed that the prepared g-C<sub>3</sub>N<sub>4</sub> exhibited a layered structure with a band gap of 2.78 eV. When the catalyst concentration is 10mg, the photocurrent intensity is 4 A, and the illumination time is 24 hours, the glucose conversion rate is 49.09 %. The active group capture experiment shows that the main active species of g-C<sub>3</sub>N<sub>4</sub> under visible light is ·O<sub>2</sub><sup>-</sup>. In this study, commercial P25 catalyst was used for photocatalytic oxidation of glucose under optimal conditions. The experimental results indicate that the catalytic oxidation performance of P25 for glucose is lower than that of layered structure g-C<sub>3</sub>N<sub>4</sub>.

## 1. Introduction

Biomass refers to all organic substances except fossil fuels, which are various organisms formed through photosynthesis through the use of atmosphere, water, soil, etc. Biomass is a renewable resource with abundant reserves. The world produces 170 billion tons of biomass every year<sup>[1]</sup>, but less than 10% is used for development and technical processing<sup>[2]</sup>. with high carbohydrates and lignin, which play an important role in the industrial utilization of biomass. It is converted into biodiesel, bioalcohol and other clean fuels to solve the problem of low efficiency of direct combustion of biomass, and dust, haze, acid rain and other environmental pollution caused by particulate matter, sulfur oxide (SO<sub>2</sub>), nitrogen oxide (NO, NO<sub>2</sub>) generated in the combustion process.

In recent years, with the continuous improvement of social demand and socio-economic development, the problem of fossil energy depletion and ecological environment deterioration has become increasingly prominent world wide, which has prompted the researchers of various countries in the world to take action and vigorously study and develop environmentally friendly and clean renewable energy. Biodiesel has attracted widespread attention due to its extensive sources, environmental friendliness, renewable and good safe<sup>[3-6]</sup>.

Glucose (C<sub>6</sub>H<sub>12</sub>O<sub>6</sub>) is the most widely distributed monosaccharide in nature, colorless crystal, with a sweet taste but not as sweet as sucrose. It is easily soluble in water, slightly soluble in ethanol, and insoluble in ether.

Its structural formula contains five hydroxyl groups and one aldehyde group, which have the properties of polyols and aldehydes. Therefore, it can undergo oxidation<sup>[7]</sup>, reduction<sup>[8]</sup>, esterification, and hydrolysis reactions<sup>[9]</sup>. Glucose is also commonly used as an important raw material in industrial production, as a reducing agent in the printing, dyeing, and leather industry. Glucose is also commonly used as a reducing agent in chemical silver plating industries such as mirror making, hot water bottle liner silver plating, and glass fiber silver plating.

Changjun Yang<sup>[10]</sup> et al. used FePz(SBu)<sub>8</sub> modified SnO<sub>2</sub> to catalyze glucose aqueous solution. The modified catalyst has enhanced light absorption, good adsorption, and significantly enhanced catalytic activity for organic acids. Thanks to the synergistic effect of FePz(SBu)<sub>8</sub> and SnO<sub>2</sub>, the glucose conversion rate is 34.2 % and the selectivity is 52.2 %, opening up a new way for the use of photocatalytic technology to catalyze the preparation of organic acids from biomass.

Lopez Sanchez, J. A<sup>[11]</sup>, et al. utilized TiO<sub>2</sub> loaded nanoparticles Ag as a catalyst and optimized the catalyst composition, substrate catalyst ratio, and reaction medium to almost completely inhibit the mineralization pathway. TiO<sub>2</sub>/Ag with a loading amount of 0.5 % had the best effect, with a selectivity of up to 98 % for partial oxidation products and small chain monosaccharide. The products were gluconic acid, arabinose, erythrose, glyceraldehyde and formic acid.

\* Corresponding author: liyan082093@163.com

## 2. Experimental part

### 2.1. Main reagents and instruments

Main reagents: cyanamide, colloidal silica, nitrogen pentahydride fluoride, glucose, high-purity oxygen, P25, acetonitrile, benzoquinone, tert-butyl alcohol, disodium ethylenediaminetetraacetic acid. Main instruments: analytical balance, photochemical reaction instrument, high performance liquid chromatograph, cold field emission scanning electron microscope, ultraviolet visible diffuse reflectance spectrometer, transmission electron microscopy, X-ray powder diffractometer, X-ray photoelectron energy, gas chromatograph.

### 2.2. Preparation of catalysts

Using cyanamide as the precursor and nano SiO<sub>2</sub> aqueous solution as the template. Weigh 3g of cyanamide and 7.50 g of silica aqueous solution, stir and mix at room temperature until the cyanamide is completely dissolved. Transfer to an oil bath and stir at 60°C for 12 hours until the water is completely evaporated. Transfer the evaporated white solid to a crucible and place it in a tube furnace. Calcine at a heating rate of 10 °C/min in a nitrogen atmosphere at 550 °C for 4 hours. After calcination, cool to room temperature, transfer the solid to a polypropylene bottle, add 12 g of NH<sub>4</sub>HF and 50 mL of water, stir thoroughly for 24 hours, remove after stirring, wash repeatedly with deionized water and ethanol several times, centrifuge, vacuum dry at 40 °C, and set aside after drying.

### 2.3. Photocatalytic oxidation of glucose

Prepare 0.1M glucose aqueous solution as a reserve solution for glucose photocatalytic oxidation experiments. Evaluate the photocatalytic activity of g-C<sub>3</sub>N<sub>4</sub> nanomaterial by photocatalytic degradation of glucose under visible light conditions. The light source is a 500W Xe lamp, which uses a filter to filter out ultraviolet light ( $\lambda < 420\text{nm}$ ), add 10mg of photocatalyst and 10ml of glucose stock solution to the photoreaction bottle, stir with magnetic force for 30 minutes, and then turn on the light to achieve adsorption desorption equilibrium between the catalyst and the substrate. After the reaction is completed, remove the reaction solution, centrifuge at 12000 r/min, and filter with a filter membrane to obtain a clear solution.

### 2.4. Free radical capture experiment

In order to explore the mechanism of photocatalytic degradation, the system conducted capture experiments and demonstrated the active species in the photocatalytic reaction through free radical capture experiments. BQ (benzoquinone), TBA (tert butanol), and EDTA-2Na (disodium ethylenediaminetetraacetic acid) captured  $\cdot\text{O}_2^-$ ,  $\cdot\text{OH}$ , and  $\cdot\text{h}^+$ , respectively. Compare the photocatalytic degradation experiment without any capture agent.

## 3. Results and discussion

### 3.1. Characterization of catalysts

#### 3.1.1 XRD analysis

The XRD results of g-C<sub>3</sub>N<sub>4</sub> is shown in figure 1. The sample exhibits two distinct diffraction peaks at both 13.1 ° and 27.7 ° positions. The peak at 13.1 ° corresponds to the (100) crystal plane of the triazine structure, and the peak at 27.7 ° corresponds to the (002) crystal plane formed by the stacking of conjugated double bonds in the aromatic system. It can be seen that the crystallinity is good, consistent with the standard card (JCPDS-87-1526).

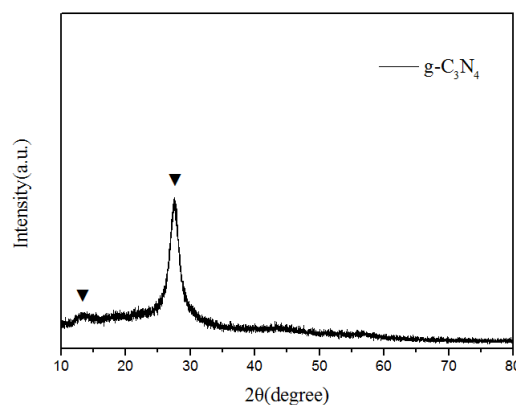


Fig. 1. XRD analysis

#### 3.1.2 Surface morphology characterization

This study synthesized g-C<sub>3</sub>N<sub>4</sub> using the hard template method, and the SEM and TEM characterization results are shown in figures 2 and 3. Figure 2 shows that the overall structure presents an amorphous block structure; At 2 μm size, the SEM image at m scale shows that after removing the template, g-C<sub>3</sub>N<sub>4</sub> is stacked by sheet structure. The layered structure increases the specific surface area of the catalyst, which increases the active site and improves the photocatalytic activity.

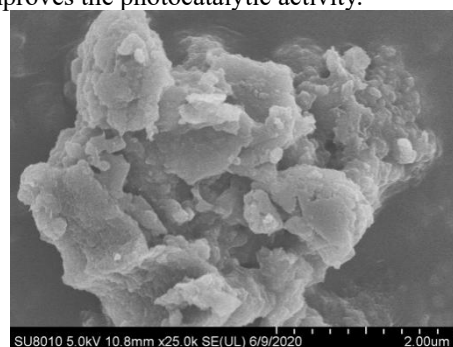
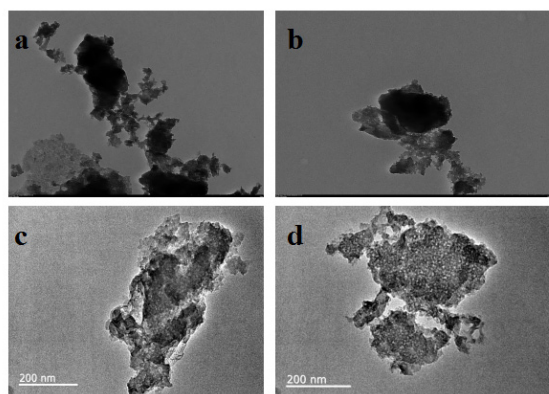


Fig. 2. SEM image of g-C<sub>3</sub>N<sub>4</sub>

The TEM diagram is shown in figure 3. Figure a and figure b show the TEM diagram at 500 nm scale. The sample as a whole shows a lamellar structure. Figure b and figure d show the TEM diagram at 200 nm scale. It can be seen that the catalyst monomer is also a graphite photo layered structure, with many active site and complete structure.



**Fig. 3.** TEM image of g-C<sub>3</sub>N<sub>4</sub>

### 3.1.3 XPS characterization results

The element analysis is carried out through XPS, and the Binding energy is corrected at C 1s (284.60). The results are shown in figure 4. Figure a shows the full spectrum, from which it can be seen that the material displays signal peaks of C, N, and O elements; Figure b shows the 1s peak of C, and it can be seen that there are two peaks at 284.8 eV and 288.2 eV, corresponding to C-C and N-C=N bonds, respectively; Figure c shows the 1s peak of N, and it can be seen that there are three peaks at 398.6 eV, 400.8 eV, and 404.2 eV, corresponding to N-C=N, N-(C)3, and C-NH bonds, respectively.

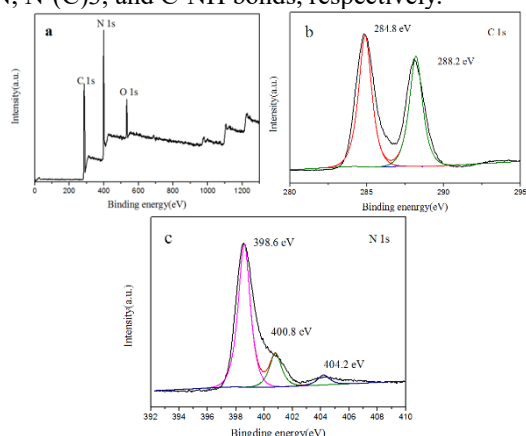


**Fig. 4.** XPS spectrum of g-C<sub>3</sub>N<sub>4</sub> (a) full XPS spectrum of g-C<sub>3</sub>N<sub>4</sub> (b) C 1s (c) N 1s (d) O 1s high-resolution spectrogram.

### 3.1.4 UV-Vis characterization results

The UV-visible spectrum is shown in figure 5.

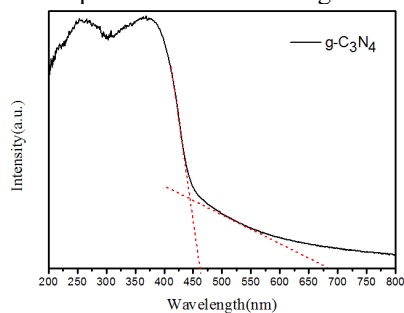


**Fig. 5.** UV-Vis image of g-C<sub>3</sub>N<sub>4</sub>

The absorption range of g-C<sub>3</sub>N<sub>4</sub> is between 200 and 460 nm, absorbing ultraviolet light and a small portion of visible light. Tangential intersections are made in the vertical and horizontal transition directions, respectively. The calculated bandgap width is approximately 2.78 eV.

### 3.2.g-C<sub>3</sub>N<sub>4</sub> photocatalytic oxidation of glucose

This study designed an orthogonal experiment to investigate the effects of different experimental conditions (such as illumination time, photocurrent intensity, and catalyst concentration) on the photocatalytic reaction. The reaction products were qualitatively analyzed using GC-MS and quantitatively analyzed using HPLC. The experimental results are shown in Figure 6.

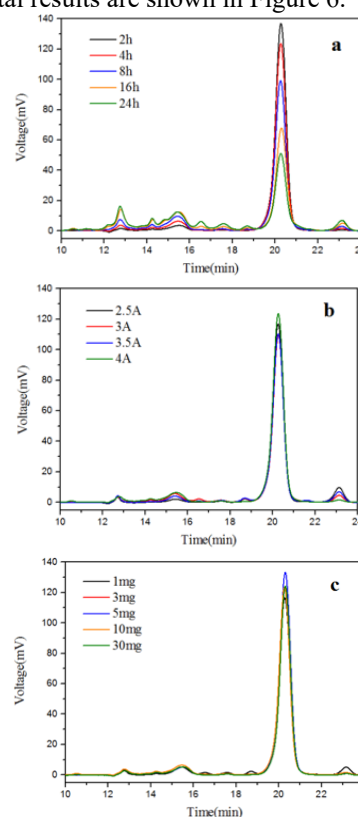


**Fig. 6.** Results of photocatalytic oxidation of glycerol under different experimental condition (a) Different lighting times (b) Different photocurrents (c) Different concentrations of g-C<sub>3</sub>N<sub>4</sub>

This study uses formulas (1) and (2) to calculate the conversion rate and selectivity of reactants. The standard curves of glycerol and reaction products were determined through liquid chromatography analysis, and the residual concentration of glucose and the concentration of products were calculated. Substituting equations (1) and (2), the conversion rates of glucose under different experimental conditions were calculated. The glucose conversion rate was 67.87% when 10mg of catalyst, 4A photocurrent intensity, and 24 hours of illumination were used. From Figure 6 (a), it can be seen that with the continuous growth of time, the types of products continue to increase, and the number of by-products also increases, resulting in a decrease in the selectivity of the reaction. Therefore, taking into account the relationship between conversion rate, selectivity, and reaction conditions (illumination time,

photocurrent intensity, and catalyst concentration), this study controlled the experimental time between 8-16 hours, and the optimal conditions for catalyzing glucose were 10 mg catalyst, The conversion rate was 49.09% when irradiated with 3.5A photocurrent for 10 h. The yield and selectivity of the reaction product under this condition are shown in Table 1, and the selectivity of the product gluconolactone is 45.16%.

$$\text{Conversion rate} = [(C_0 - C_{GC}) / C_0] \times 100\% \quad (1)$$

$$\text{Yield} = (C_{\text{product}} / C_0) \times 100 \quad (2)$$

**Table 1.** Result of glucose oxidation reaction catalyzed by 10 mg catalyst under 3.5 A for 10 h.

Product	Yield	Selectivity
5-hydroxymethylfurfural	7.18 %	14.63 %
D-arabinose	6.21 %	12.65 %
lactose	0.87 %	1.77 %
gluconolactone	22.17 %	45.16 %

In the formula,  $C_0$  is the initial concentration of the reactant,  $C_{GC}$  is the residual concentration of the reactant after the reaction is completed, and  $C_{\text{product}}$  is the concentration of the product after the reaction is completed. The results of its products are shown in Table 1, and the selectivity of gluconolactone under this condition is as high as 45.16 %.

In addition, this study used commercial P25 catalyst for photocatalytic oxidation of glucose under the optimal experimental conditions. The performance of P25 for catalytic oxidation of glycerol is lower than  $g\text{-C}_3\text{N}_4$ , and the conversion rate of commercial P25 is 31.33 %.

### 3.3. Photocatalytic mechanism

The photocatalytic mechanism results is shown in figure 7.

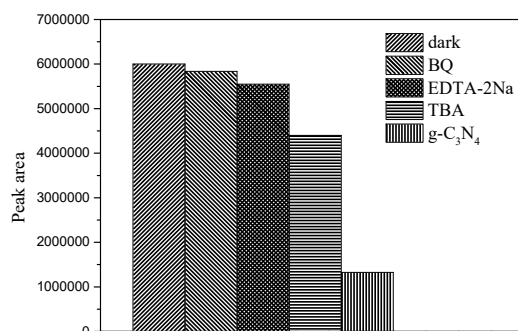


**Fig. 7.** Peak area of glycerol with different capture reagents added in the reaction

From the figure, it can be seen that in the dark state, without the light source driving, glucose does not react. When the hole trapping agent EDTA-2Na was added, the reaction was almost terminated, indicating that after the holes were captured, the main active groups in the system were lost, greatly reducing the photocatalytic activity. Holes played a dominant role in this reaction. When BQ and TAB are added, the activity of the reaction is greatly reduced, indicating that the reaction system catalyzes the substrate through the synergistic effect of  $\cdot\text{O}_2^-$  and  $\cdot\text{OH}$ . From the peak area graph, it can be seen that the dominant position of  $\cdot\text{O}_2^-$  is much higher than that of  $\cdot\text{OH}$ .

## 4. Conclusion

This study successfully synthesized a layered structure  $g\text{-C}_3\text{N}_4$  and characterized its crystal morphology, optical and electrochemical properties. And use it to catalyze the oxidation of glucose. We studied the effects of different experimental conditions on the reaction results and explored the reaction mechanism. Qualitative and quantitative analysis was conducted on the reaction products. The highest conversion rate of glucose is 67.87 %, which is higher than commercial  $\text{TiO}_2$ . Under optimal conditions, after irradiation with 10ml glucose aqueous solution, 10mg catalyst, and 3.5A photocurrent for 10 hours, the glucose conversion rate was 49.09%, and the selectivity for gluconolactone was 45.16%.

## References

1. Corma A., Iborra S., Velty A. Chem. Rev. 107(6), 2411-2502, (2007).
2. Sheldon R. A., Green Chem. 16(3), 950-963, (2014).
3. Li Z. H., Yi Z. G., Li Z. S., Zou Z. G. Solar RRL. 5(6), (2021).
4. Wu X. J., Luo N. C., Xie S. J., Wang Y. Chem. Soc. Rev. 49(17), 6198-6223, (2020).
5. Wang M., Wang F., Zhou H. R. Acc. Chem. Res. 56(9), 1059-1069, (2023).
6. Xue Z. H., Luan D. Y., Zhang H. B. JOULE. 6(1), 92-133, (2022).
7. Ghonim A. M., El-Anadouli B. E., Saleh M. M. Elec. Acta. 114, 713-719, (2013).
8. Findlay A., Williams V. H. T. Far. Soc. 17(02), 0453-0456, (1992).
9. Omeara D., Shepherd D. M. J. Chem. Soc., 3377-3380, (1957).
10. Zhang Q., Ge Y., Yang C., Zhang B., Deng K. Green Chem. 21(18), 5019-5029, (2019).
11. Da Via L., Recchi C., Davies T. E., Greeves N., Lopez-Sanchez J. A. Chem. Cat. Chem. 8(22), 3475-3483, (2016).